AMERICAN SOCIETY FOR MICROBIOLOGY | mBio®

RESEARCH ARTICLE
Applied and Environmental Science

Streamlined Genetic Manipulation of Diverse *Bacteroides* and *Parabacteroides* Isolates from the Human Gut Microbiota

Leonor García-Bayona,[a] Laurie E. Comstock[a]

[a]Division of Infectious Diseases, Brigham and Women's Hospital, Harvard Medical School, Boston, Massachusetts, USA

ABSTRACT Studies of the gut microbiota have dramatically increased in recent years as the importance of this microbial ecosystem to human health and disease is better appreciated. The *Bacteroidales* are the most abundant order of bacteria in the healthy human gut and induce both health-promoting and disease-promoting effects. There are more than 55 species of gut *Bacteroidales* with extensive intraspecies genetic diversity, especially in regions involved in the synthesis of molecules that interact with other bacteria, the host, and the diet. This property necessitates the study of diverse species and strains. In recent years, the genetic toolkit to study these bacteria has greatly expanded, but we still lack a facile system for creating deletion mutants and allelic replacements in diverse strains, especially with the rapid increase in resistance to the two antibiotics used for genetic manipulation. Here, we present a new versatile and highly efficient vector suite that allows the creation of allelic deletions and replacements in multiresistant strains of *Bacteroides* and *Parabacteroides* using a gain-of-function system based on polysaccharide utilization. These vectors also allow for easy counterselection independent of creating a mutant background strain, using a toxin from a type VI secretion system of *Bacteroides fragilis*. Toxin production during counterselection is induced with one of two different molecules, providing flexibility based on strain phenotypes. This family of vectors greatly facilitates functional genetic analyses and extends the range of gut *Bacteroidales* strains that can be genetically modified to include multiresistant strains that are currently genetically intractable with existing genetic tools.

IMPORTANCE We have entered an era when studies of the gut microbiota are transitioning from basic questions of composition and host effects to understanding the microbial molecules that underlie compositional shifts and mediate health and disease processes. The importance of the gut *Bacteroidales* to human health and disease and their potential as a source of engineered live biotherapeutics make these bacteria of particular interest for in-depth mechanistic study. However, there are still barriers to the genetic analysis of diverse *Bacteroidales* strains, limiting our ability to study important host and community phenotypes identified in these strains. Here, we have overcome many of these obstacles by constructing a series of vectors that allow easy genetic manipulation in diverse gut *Bacteroides* and *Parabacteroides* strains. These constructs fill a critical need and allow streamlined allelic replacement in diverse gut *Bacteroidales*, including the growing number of multiantibiotic-resistant strains present in the modern-day human intestine.

KEYWORDS *Bacteroides*, microbiota, mutant construction, vectors

The human gut microbiota is a diverse and dense microbial ecosystem that plays an essential role in health and development (1, 2). Large-scale metagenomic, metatranscriptomic, and metabolomic studies are revealing the molecular repertoire of this complex community (3, 4), yet functional genetic, phenotypic, and mechanistic studies

Citation García-Bayona L, Comstock LE. 2019. Streamlined genetic manipulation of diverse *Bacteroides* and *Parabacteroides* isolates from the human gut microbiota. mBio 10:e01762-19. https://doi.org/10.1128/mBio.01762-19.

Editor Katherine P. Lemon, The Forsyth Institute

Copyright © 2019 García-Bayona and Comstock. This is an open-access article distributed under the terms of the Creative Commons Attribution 4.0 International license.

Address correspondence to Laurie E. Comstock, lcomstock@rics.bwh.harvard.edu.

This article is a direct contribution from a Fellow of the American Academy of Microbiology. Solicited external reviewers: Jean-Marc Ghigo, Institut Pasteur; Eugene Chang, University of Chicago.

Received 3 July 2019
Accepted 12 July 2019
Published 13 August 2019

lag far behind and are essential to understand the complex interactions within this microbial ecosystem and how these microbes interface with their host (3, 4).

The *Bacteroidales* are an order of Gram-negative bacteria that includes the abundant gut genera *Bacteroides*, *Parabacteroides*, and *Prevotella*, which collectively include more than 55 identified human gut species (5, 6). These bacteria display remarkable stability and substantial resilience to temporary perturbations, with many strains colonizing for decades (7–9). The majority of genetic and phenotypic studies of the gut *Bacteroidales* have analyzed only three strains: *Bacteroides fragilis* NCTC 9343, *B. fragilis* 638R, and *B. thetaiotaomicron* VPI 5482 (10, 11). However, *Bacteroidales* species have remarkable genome plasticity, with extensive within-species genetic diversity and metabolic abilities and large pangenomes (6, 12, 13). Many of the regions involved in the synthesis of outer surface and secreted molecules that are likely to interface with other microbes or the host are in heterogeneous regions of a species (12, 14–20). This heterogeneity highlights the need for functional genetic studies of diverse human isolates.

Bacteroides species are intrinsically resistant to many of the antibiotics commonly used in the laboratory and now display increasing resistance to many antibiotics used in clinical settings (21–28). Due to pervasive horizontal gene transfer of antibiotic resistance genes, many *Bacteroides* and *Parabacteroides* isolates from American and European subjects now display resistance to tetracycline and erythromycin, the two commonly used antibiotics for genetic selection (25, 29–31). Chloramphenicol and cefoxitin resistance genes have been used to select for replicative plasmids in *B. fragilis*, *B. vulgatus*, and *B. thetaiotaomicron* strains (29, 32, 33) and sometimes function for chromosomal integrations in select genetic backgrounds (29, 31, 34–36). However, cefoxitin and carbapenems are clinically relevant antibiotics and should ideally be avoided in the laboratory to prevent the spread of resistance genes (37).

Construction of markerless gene knockouts or other types of mutations in bacteria can be carried out through lambda red recombineering or CRISPR-Cas9-based systems (38–40). However, these methods often require strain-specific modifications; rely on efficient transformation, which is often impossible or very inefficient in *Bacteroidales*; and may lead to off-target mutations (38–42). Allelic replacement in *Bacteroides* is a two-step process. First, a suicide vector is transferred via conjugation and integrated into the chromosome via homology-based recombination of regions flanking the target deletion and selected via a gain-of-function phenotype, typically antibiotic resistance. This limits the tractable strains to those sensitive to erythromycin or tetracycline and therefore excludes a large number of isolates. Genomes that undergo double-crossover events result in the excision of the vector and typically are identified by one of three different methods. The first is replica plating, which has the advantages that there is no need for a genetic mutation to first be made in the background strain and that the resulting strains therefore have no additional underlying genetic mutation. The disadvantage is that this is a more labor-intensive and slow process, requiring the analysis of thousands of colonies. A second method uses counterselection where a genetic mutation of *thyA*, encoding thymidylate synthetase, is made in the background strain (64). *thyA* is placed on the suicide vector, and double-crossover resolvents are selected by plating on trimethoprim, which kills *thyA*-positive cells. A third method is similar to the *thyA* procedure but requires the creation of a background mutant strain of *tdk*, encoding thymidine synthase, with the selection of resolvents by plating on 5-fluoro-2′-deoxyuridine (50). Other counterselection systems readily used in proteobacteria, such as *sacB* and *rpsL* (42), do not function in *Bacteroides*. Recently, a new counterselection marker was implemented based on an allele of the phenylalanyl-tRNA synthetase (*pheS**), lethal in the presence of *p*-chloro-phenylalanine (*p*-Cl-Phe) (43). This system functions in some strains but not others, requires growth on minimal medium, and often results in significant background growth.

Here, we created a new vector family for genetic modifications in gut *Bacteroidales*. These vectors allow easy allelic replacement without first making a mutant background strain for counterselection. In addition, we created vectors where the gain of function is the ability to utilize a polysaccharide rather than antibiotic resistance, greatly

increasing the range of strains that can be genetically manipulated to include multiresistant strains. We provide numerous examples of these vectors functioning in diverse *Bacteroidales* species, regardless of the antibiotic resistance profile.

RESULTS AND DISCUSSION

An inulin selection cassette for use in antibiotic-resistant *Bacteroidales* strains. Analyses of recent human fecal isolates of *Bacteroidales* with interesting phenotypes revealed that many are resistant to both tetracycline and erythromycin (60, 65) and therefore are not amenable to genetic manipulation using available genetic tools for these bacteria. We evaluated tetracycline and erythromycin resistance among 120 *Bacteroides* strains from our collection isolated between 2009 and 2011 from the stool of 15 healthy U.S.-resident adults with no history of gastrointestinal diseases (Fig. 1A) (18). For each subject/ecosystem (named CL01 to CL15), the stated numbers of *Bacteroides* isolates analyzed are listed (Fig. 1A) (18). On average, 59% of the isolates from these combined ecosystems are resistant to erythromycin, and 74% are resistant to tetracycline, while 51% are doubly resistant. In particular, 63% of *B. ovatus* and 67% of *B. thetaiotaomicron* isolates from these ecosystems are doubly resistant. The incidence of resistance varies widely depending on the ecosystem (Fig. 1A), with isolates from ecosystems CL03, CL08, and CL14 displaying low levels of double resistance, while ecosystems CL01, CL05, CL07, CL11, and CL12 are almost entirely composed of doubly resistant isolates. These results are consistent with other reports of widespread resistance to tetracycline and erythromycin in recent *Bacteroides* and *Parabacteroides* isolates (22, 23, 31).

To overcome the genetic intractability of these strains, we designed a nonantibiotic selection marker that confers the ability to utilize inulin as a carbon source. To test if inulin selection would be useful in the doubly antibiotic-resistant isolates, we screened 57 of these strains for growth on defined, minimal inulin medium (M9S-inulin) (Fig. 1B) and observed that 28 (49%) are inulin utilizers. Excluding *B. fragilis* and *B. uniformis*, the majority of doubly resistant isolates of other *Bacteroides* species (72%) lack the ability to grow on inulin and are therefore theoretically amenable to inulin selection.

The choice of conferring inulin utilization for gain-of-function selection of cointegrates is based on the fact that inulin is a simple linear polysaccharide ([β1,2] fructose polymer) that does not require surface digestion (20, 44). Therefore, the inulin utilization locus is smaller than most polysaccharide utilization loci (PULs), which typically span 20 to 60 kb (10, 45, 46), and includes several dispensable genes (Fig. 1C) (20, 44, 47). The absence of extracellular digestion prevents background growth of nontransconjugant cells (44). We constructed a three-gene inulin utilization cassette from the inulin locus of *B. ovatus* ATCC 8483. It comprises genes encoding the outer membrane SusC-like TonB-dependent inulin transporter (*BACOVA_04505*), its associated inulin-binding surface lipoprotein (SusD-like; *BACOVA_04504*), and the periplasmic glycoside hydrolase (*BACOVA_04501*) (44, 48) (Fig. 1C). The three genes were placed under the control of a strong constitutive promoter from the *B. thetaiotaomicron* VPI 5482 housekeeping sigma factor P_{BT1311} (49). This inulin selection cassette (6.7 kb) was placed into pNBU2 (50), replacing the erythromycin cassette, to create pLGB28 (Fig. 1D). pNBU2 is a *pir*-dependent suicide vector which replicates in certain *Escherichia coli* strains but must integrate for maintenance in *Bacteroides* species. pNBU2 encodes an IntN2 tyrosine recombinase that catalyzes the integration of the vector at a chromosomal *attBT2* site (50, 51). Most *Bacteroides* strains have two *attBT2* sites, located at the 3′ end of the two $tRNA^{Ser}$ genes (51). Double-integration events are not expected, as the integration of the plasmid disrupts the tRNA gene (51).

We conjugally transferred pLGB28 into 17 doubly resistant *Bacteroides* and *Parabacteroides* strains unable to utilize inulin as a sole carbon source. We obtained inulin-utilizing integrants for 14 of these strains from nine different species (Fig. 1E and F). Four strains displayed some background growth, which required restreaking of single colonies for isolation. As inulin selection is not bactericidal, we recommend that integrants always be restreaked for isolation. For the majority of strains, there were

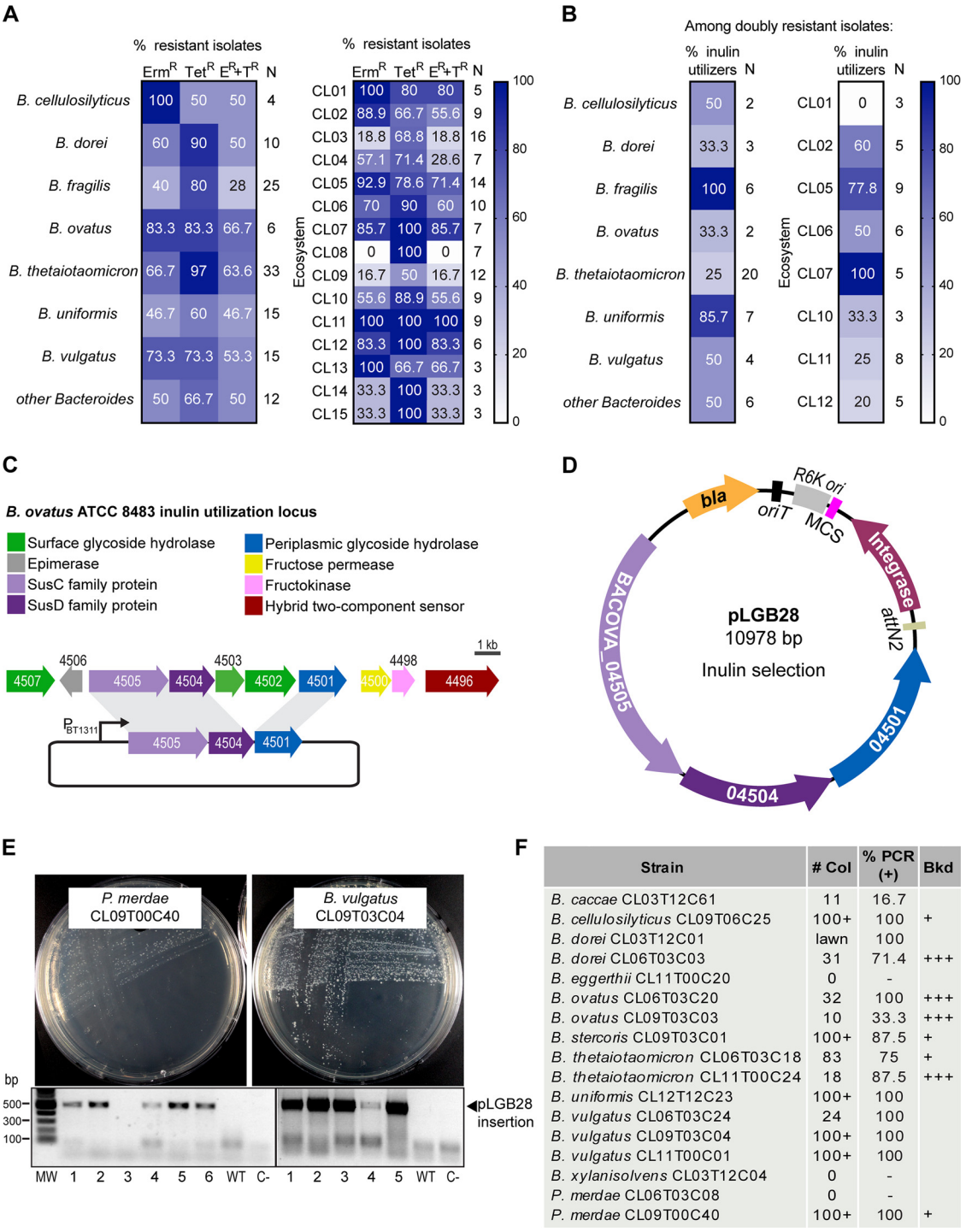

Strain	# Col	% PCR (+)	Bkd
B. caccae CL03T12C61	11	16.7	
B. cellulosilyticus CL09T06C25	100+	100	+
B. dorei CL03T12C01	lawn	100	
B. dorei CL06T03C03	31	71.4	+++
B. eggerthii CL11T00C20	0	-	
B. ovatus CL06T03C20	32	100	+++
B. ovatus CL09T03C03	10	33.3	+++
B. stercoris CL09T03C01	100+	87.5	+
B. thetaiotaomicron CL06T03C18	83	75	+
B. thetaiotaomicron CL11T00C24	18	87.5	+++
B. uniformis CL12T12C23	100+	100	
B. vulgatus CL06T03C24	24	100	
B. vulgatus CL09T03C04	100+	100	
B. vulgatus CL11T00C01	100+	100	
B. xylanisolvens CL03T12C04	0	-	
P. merdae CL06T03C08	0	-	
P. merdae CL09T00C40	100+	100	+

FIG 1 A minimal inulin utilization locus can be used for selection of integrants in many *Bacteroidales* species. (A) Percentage of tetracycline- and erythromycin-resistant *Bacteroides* strains from the Comstock laboratory ecosystems strain collection. Numbers in the right column (N) indicate the number of strains tested. (B) Percentage of inulin utilizers from the doubly resistant (Tet^r Erm^r) *Bacteroides* strains. Numbers in the right column (N) indicate the number of strains tested. Ecosystems with fewer than three doubly resistant strains were excluded. (C) Inulin utilization locus of *B. ovatus* ATCC 8483. P_{BT1311} is the strong constitutive promoter from the *BT_1311* sigma factor of *B. thetaiotaomicron* VPI 5482 used to drive the expression of the three-gene inulin utilization locus. (D) Integration vector pLGB28 integrates at chromosomal *attBT2* sites and allows for inulin utilization selection. *bla*, β-lactamase gene conferring ampicillin and carbenicillin resistance in *E. coli* S17; *oriT*, RP4 origin of transfer; RK6, replication origin in *E. coli* λ*pir*; MCS, multiple-cloning site; Integrase, IntN2 from NBU2; *attN2*, recognition and integration sequence. (E) Growth of the indicated strains on M9S-inulin plates to select for integration of pLGB28. Ethidium bromide-stained agarose gels show PCR amplification of the 500-bp fragment corresponding to integration of pLGB28 at *attBT2*. Six clones are shown per strain. WT, wild type; C−, no-DNA control; MW, molecular weight marker (Quick-Load Purple 1-kb Plus DNA ladder; NEB). (F) Results of the conjugation of pLGB28 into 17 different doubly resistant (Tet^r Erm^r), inulin-nonutilizing *Bacteroides* and *Parabacteroides* strains from panel B. # Col, number of colonies

(Continued on next page)

numerous integrants with little or no background growth. Notably, we easily obtained transconjugants in *Parabacteroides merdae* CL09T00C40 (*Pm*CL09), indicating that these protocols and vector series can be used in different families of *Bacteroidales*. Interestingly, both *attBT2* sites in *Pm*CL09 have two base pair differences relative to the *attBT2* sequence of pNBU2 and *Bacteroides* chromosomes (51), indicating some promiscuity for IntN2-mediated recombination. To verify integration at the *attBT2* sites, we designed PCR primers that anneal upstream of the recombination site (forward primer) and inside pNBU2 (reverse primer). Most integrates in the majority of strains had the insertion at one of the two $tRNA^{Ser}$ loci. However, in *B. ovatus* CL09T03C03 and *B. caccae* CL03T12C61, PCR revealed that most inulin-utilizing clones did not have an insertion of the plasmid in $tRNA^{Ser}$. Importantly, these data show that selection of integrants using inulin selection is a feasible alternative to antibiotic selection for most doubly resistant *Bacteroides* species.

The aTC-inducible ssBfe1 is a highly effective counterselection system. Two-step allelic exchange (Fig. 2A) involves an intermediate cointegrate step where the suicide vector containing the genes for positive selection is integrated into the chromosome at the target site, followed by growth in nonselective medium and plating with selection for cells that have undergone the second recombination (cross-out) event. Selection of double-crossover resolvents using a lethal toxin encoded on the plasmid to kill cointegrates should be an effective counterselection system. Three essential features of such a counterselection system are the low frequency of toxin-resistant escapees, broad host range of toxicity, and tight regulation of the toxin (produced only during the counterselection step). The highly toxic effector Bfe1 from the *B. fragilis* 638R type VI secretion system (T6SS), which mediates antibacterial antagonism against a wide range of *Bacteroidales* species (52), was chosen for counterselection. Lim et al. showed that Bfe1 can be endogenously expressed in *B. thetaiotaomicron* VPI 5482 and kill this strain when targeted to the periplasm using an N-terminal localization signal sequence (ssBfe1) (53). When placed under the tightly regulated anhydrotetracycline (aTC)-inducible promoter developed for *Bacteroides* by Lim et al. (Fig. 2B), periplasmic Bfe1 expression leads to rapid cell death, with no evidence of escapees (53). Furthermore, although *Bacteroides* species have been shown to commonly harbor islands of immunity genes to multiple T6SS effectors (54), the *bfi1* (*BF638R_1987*) immunity gene to Bfe1 (52) is absent from these islands. tBLASTn searches of 724 available *Bacteroides* and *Parabacteroides* genomes revealed that only 35 *B. fragilis* strains have *bfi1*, all of them as part of a T6SS cluster containing *bfe1* (complete genomes and whole-genome shotgun contigs in GenBank, along with our in-house-sequenced strains).

As this system met all the criteria for successful counterselection, we made a counterselection suicide vector. Starting from the aTC-inducible pNBU2_erm-TetR-P1T_DP-GH023 integration vector (53), we removed the *attBT2* site and its cognate integrase gene, necessitating integration by homologous recombination. The *ssbfe1* cassette was added under the control of the aTC promoter. The multiple-cloning site for insertion of DNA for homology-based recombination was retained (pLGB13) (Fig. 2B and C).

To test pLGB13 for creating chromosomal deletions, we made a construct to delete the 36-kb GA1 T6SS locus (*HMPREF1057_01517* to *HMPREF1057_01551*) of *B. finegoldii* CL09T03C10 (*Bfi*CL09) (Fig. 2D). All colonies obtained after counterselection (on aTC selection plates) were erythromycin sensitive, indicating loss of the vector. PCR verification of eight clones indicated that six were wild-type revertants and that two had the desired 36-kb deletion (clones 2 and 7). To further verify this large deletion, we designed a second set of primers that anneal to the chromosome in the regions

FIG 1 Legend (Continued)
obtained per 13.75 ml of mating culture mix; %PCR (+), percentage of clones that were PCR positive as described above for panel E; Bkd, amount of background growth in the inulin selection plate; +, slight hazy background with distinct colonies (as observed in panel E, left); +++, strong background growth (as observed in Fig. 3B, left).

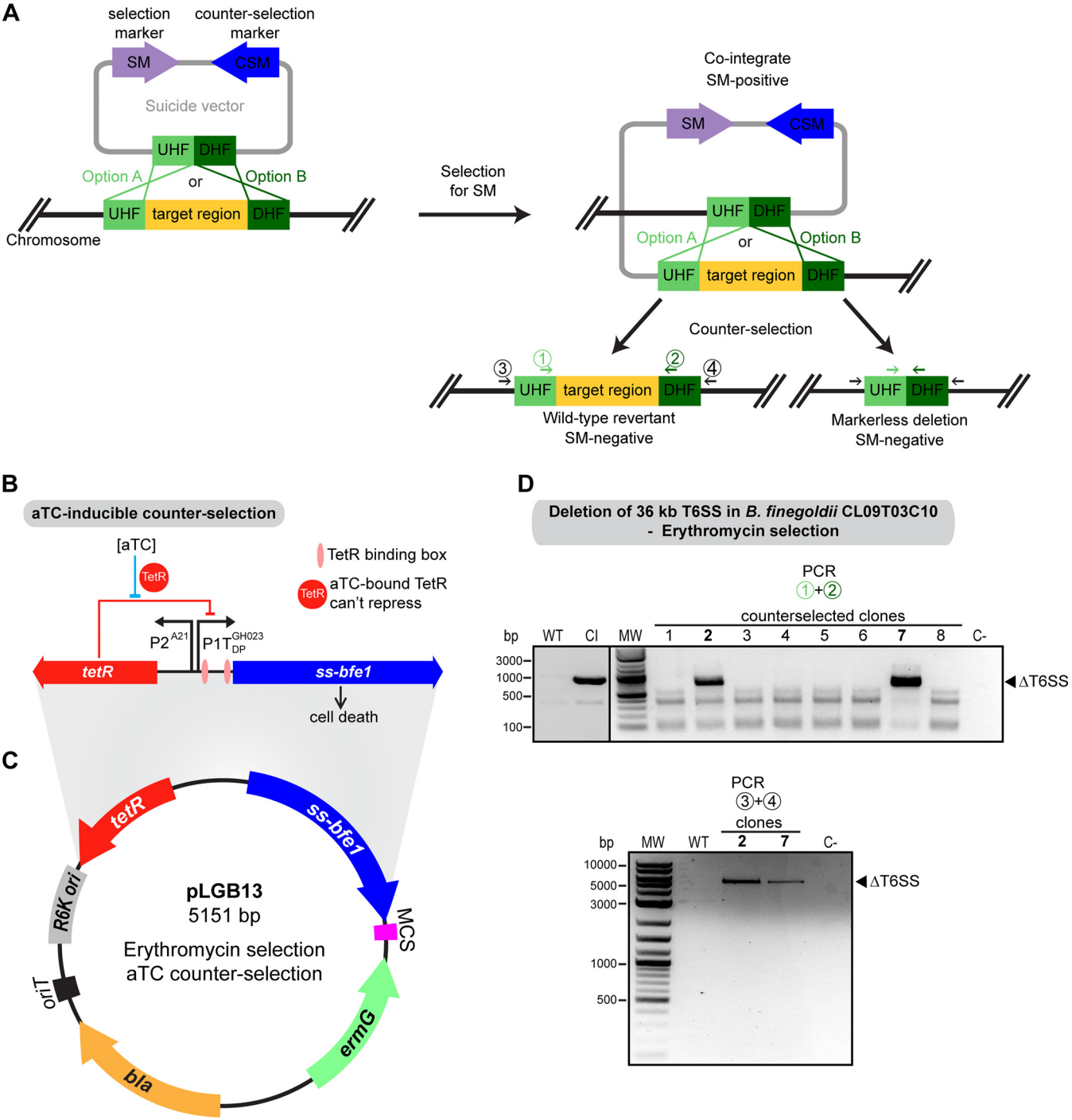

FIG 2 Bfe1-based counterselection induced by aTC is highly effective. (A) Diagram of the two-step allelic replacement process. UHF, upstream homology flank; DHF, downstream homology flank. (B) aTC-inducible ssBfe1 counterselection cassette (53). (C) Vector pLGB13. *bla*, OriT, RK6, and MCS are described in the Fig. 1D legend. *ermG*, erythromycin resistance gene. (D) PCR verification of the counterselected clones for deletion of the 36-kb T6SS region of *Bfi*CL09. WT, wild type; CI, cointegrate; C−, no-DNA control; MW, molecular weight marker. (Top) PCR using primers 1 and 2; (bottom) PCR using primers 3 and 4, as indicated in panel A.

upstream and downstream of the flanking DNA cloned into pLGB13 (primers 3 and 4) (Fig. 2A). A PCR with these primers in clones 2 and 7 yielded the expected amplicon size (5.2 kb), whereas a cointegrate or a wild-type revertant would produce no amplicon (Fig. 2D). This pLGB13 counterselection system has now been successfully used in the laboratory to make deletions and allelic replacements in strains of *B. uniformis*, *B. thetaiotaomicron*, and *B. vulgatus*.

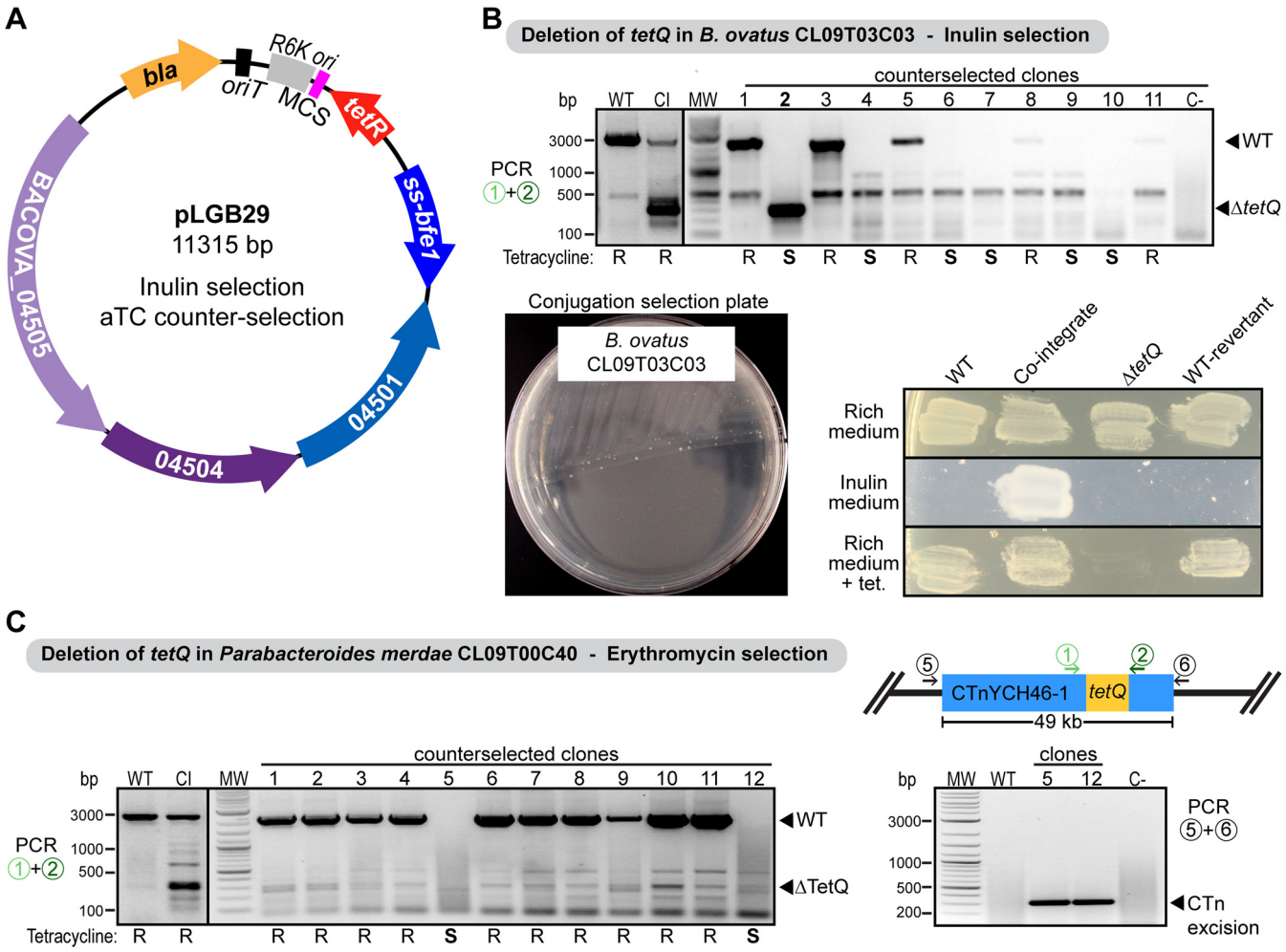

FIG 3 Deletion of the tetracycline resistance gene *tetQ*. (A) Allelic replacement vector pLGB29, using inulin selection for cointegrates. *bla*, *oriT*, RK6, and MCS are described in the Fig. 1D legend. (B) PCR verification and growth on plates of the counterselected clones for the *tetQ* deletion in *Bo*CL09. An inulin selection plate for the mating of *Bo*CL09T03C03, using homology-based integration of pLGB29 containing 1 kb of DNA on each side of the *tetQ* gene, is shown. S, sensitive; R, resistant. (C, left) Ethidium bromide-stained agarose gel showing PCR amplicons of the resolvent for the *tetQ* deletion in *Pm*CL09 using pLGB13 (erythromycin sensitive). (Right) PCR amplicon to verify excision of the whole CTnYCH46-1 (*HMPREF1078_01847* to *HMPREF1078_01893*). Primers anneal upstream and downstream of the 49-kb conjugative transposon. WT, wild type; Cl, cointegrate. C−, no-DNA control; MW, molecular weight marker.

pLGB13 requires that the strain to be mutated is erythromycin sensitive. To extend this counterselection system to erythromycin-resistant strains, we replaced *ermG* of pLGB13 with the inulin utilization cassette, creating plasmid pLGB29 (Fig. 3A). As a proof of concept for inulin selection with homology-based recombination, we cloned into pLGB29 the 1-kb regions upstream and downstream of the *tetQ* tetracycline resistance gene of *B. ovatus* CL09T03C03 (*Bo*CL09) (*AA414_04155*). Cointegrates were obtained for *Bo*CL09 (Fig. 3B); however, there was background growth such that clones needed to be streaked onto inulin plates twice to obtain true cointegrates. We verified the cointegrates using PCR primers that anneal within the homology flanks (depicted in Fig. 2A as primer pair 1 and 2), such that amplification from the cointegrate should yield both the wild-type *tetQ* band (2.2 kb) as well as the shorter product representing the deletion (300 bp) (Fig. 3B).

For comparison of inulin selection against traditional erythromycin selection, we cloned the same 1-kb regions upstream and downstream of *tetQ* into pLGB13 (erythromycin selection) to delete this gene in *Pm*CL09 (erythromycin sensitive; *HMPREF1078_01857*). Cointegrates of *Bo*CL09ΩpLGB29 (inulin) or *Pm*CL09ΩpLGB13 (erythromycin) were grown in nonselective broth and plated onto medium containing 40 ng/ml aTC. None of the aTC-selected colonies grew on either inulin (*Bo*CL09) or

erythromycin (*Pm*CL09), indicating plasmid excision. However, PCR analysis and growth on plates containing tetracycline, whose resistance is encoded by the targeted deletion, indicated that most clones were wild-type revertants (Fig. 3B and C). In 1 of 30 resolvents tested for *Bo*CL09, we identified a mutant that produced the expected 300-bp PCR band corresponding to the *tetQ* deletion (clone 2) (Fig. 3B). Interestingly, five resolvents displayed no deletion band or the wild-type band (clones 4, 6, 7, 9, and 10) (Fig. 3B). Inspection of the genomic context of the *tetQ* gene in both strains revealed that it is part of a 49-kb conjugative transposon (CTn) with 99% sequence identity to CTnYCH46-1 that belongs to the CTn*341* family (55). The excision and transfer of CTn*341* (and CTnYCH46-1) are induced by tetracycline (and its derivative aTC), mediated through the two-component regulatory system RteAB (56). Therefore, selection using aTC induced the excision of the whole CTnYCH46-1 during counterselection. We observed a similar phenomenon in *Pm*CL09, where the majority of colonies after counterselection were wild-type revertants and two were CTnYCH46-1 excisions (clones 5 and 12) (Fig. 3C). We used PCR with primers annealing upstream and downstream of this 49-kb element and confirmed the excision of CTnYCH46-1 (*HMPREF1078_01847* to *HMPREF1078_01893*) in these clones (Fig. 3C). Therefore, although the aTC-ssBfe1 cassette is highly efficient for counterselection, it is not ideal for deletion of genes contained on tetracycline-inducible CTns. Since aTC induction also precludes the use of tetracycline as a selection marker, which would be desired in tetracycline-sensitive erythromycin-resistant strains, we devised a rhamnose-inducible alternative to be used in a tetracycline selection vector (pLGB30) (Fig. 4B) or an inulin selection vector (pLGB31) (Fig. 4F), described below. pLGB31 can also be used for allelic replacement of genes contained in the tetracycline-inducible CTn.

The rhamnose-inducible ssBfe1 system. Mimee et al. showed that the RhaR (BT_3768) transcriptional activator from *B. thetaiotaomicron* VPI 5482 can be used to drive robust activation of the *BT_3763* (*rhaK*) promoter (Fig. 4A) (57, 58). We placed s*sbfe1* under the control of this promoter cassette, creating suicide vectors pLGB30 (tetracycline selection) (Fig. 4B) and pLGB31 (inulin selection) (Fig. 4F). As some strains of *Bacteroidales* are able to grow with rhamnose as the sole carbon source and others are not, we analyzed whether this system would function in strains with each of these phenotypes. We first tested this system in *B. fragilis* NCTC 9343 (*Bf*9343) (Tet^s), which does not have the ability to grow using rhamnose as the sole carbon source and whose genome does not harbor a described rhamnose utilization locus. Using pLGB30, we made a construct to delete the gene encoding the antimicrobial toxin BfUbb (BF9343_3779), which inhibits the growth of other *B. fragilis* strains (59). Despite the inability of *Bf*9343 to utilize rhamnose, the system drove the expression of *ssbfe1* to high-enough levels that only double-crossover resolvents grew on the rhamnose counterselection plates, and all these colonies lost pLGB30, as they were not tetracycline resistant. Therefore, *Bf*9343 cells have some ability to take up rhamnose, although they do not have a described RhaT permease (58). PCR analysis of four resolvents identified three with the correct *ubb* deletion (clones 2, 3, and 4) (Fig. 4C). We verified this deletion phenotypically by testing for killing activity using the spot agar overlay assay (Fig. 4C). Wild-type *Bf*9343 produced a large zone of growth inhibition for the two tested BfUbb-sensitive strains, whereas the *Bf*9343 Δ*ubb* strain lost this ability. A small inhibition zone was observed, corresponding to the size of the original bacterial spot, demonstrating that *Bf*9343 produces an additional antimicrobial toxin, as is typical of *B. fragilis* strains (59, 60). These analyses show that pLGB30 allows for easy creation of double-crossover mutants in erythromycin-resistant strains where tetracycline selection of cointegrates is necessary.

To determine if this vector can be widely used in non-rhamnose-utilizer strains, we carried out BLAST searches of all 724 available *Bacteroides* and *Parabacteroides* genomes. We used as queries the rhamnose symporter (*BT_3765*), rhamnulose-1-phosphate aldolase (*BT_3766*), and rhamnulose kinase (*BT_3763*) genes from *B. thetaiotaomicron* VPI 5482 (58). All *Bacteroides* and *Parabacteroides* genomes from all

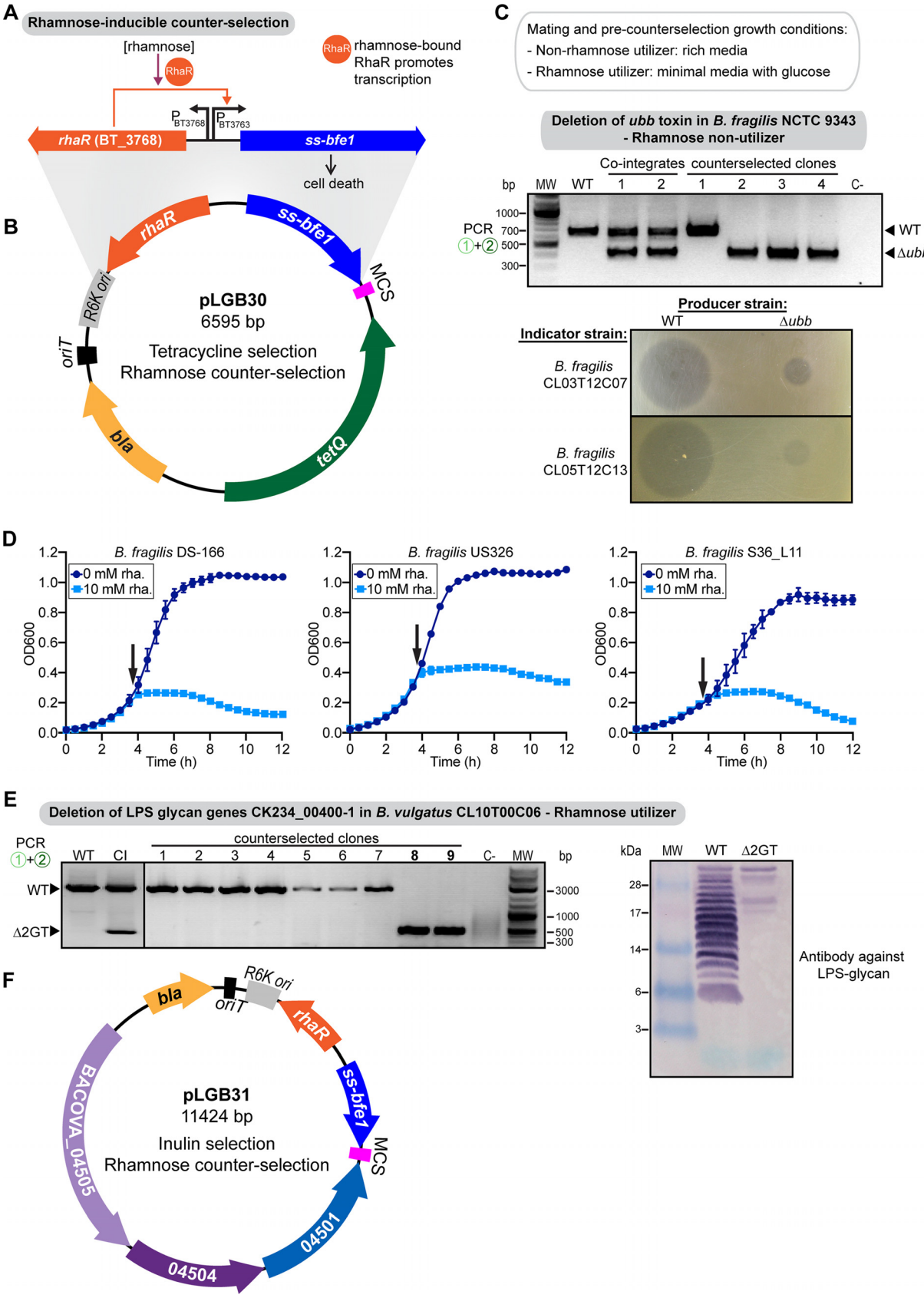

FIG 4 Bfe1-based counterselection induced by rhamnose. (A) Rhamnose-inducible ssBfe1 counterselection cassette. (B) Allelic replacement vector pLGB30 using tetracycline selection of cointegrates. *bla*, *oriT*, RK6, and MCS are described in the Fig. 1D legend. *tetQ*, tetracycline

(Continued on next page)

species had >90% identity hits, indicating that rhamnose utilization is a conserved trait. The exceptions were all 167 strains of *B. fragilis*. To establish if rhamnose induction of ssBfe1 would function for counterselection in other strains of *B. fragilis*, which homology-based searches suggest are also unable to utilize rhamnose, we made a pNBU2-derivative chromosomal integration vector carrying the RhaR-*ssbfe1* cassette. We integrated this construct into three *B. fragilis* strains and monitored their growth with or without added rhamnose (Fig. 4D). For all three strains, rhamnose addition led to a very rapid growth arrest, with no evidence of resumed growth up to 8 h after toxin induction. Therefore, even though *B. fragilis* strains are unable to utilize inulin as a sole carbon source, this rhamnose-inducible toxin system functions broadly in this species.

Next, we tested this counterselection system in a rhamnose-utilizing strain, *B. vulgatus* CL10T00C06 (*Bv*CL10). Unlike *B. fragilis*, *Bo*CL09 has a rhamnose permease as well as a rhamnose two-component signaling system, likely leading to induction of the *rhaK* promoter at much lower concentrations of rhamnose than for a rhamnose nonutilizer. Therefore, all steps prior to counterselection were performed using defined M9S-glucose medium, as small amounts of rhamnose in BHIS plates or supplemented basal medium (SBM) broth could induce premature expression of the toxin. We made a construct in pLGB30 to delete the genes *CK234_00400* and *CK234_00401* (*CK234_00400-1*). These genes encode glycosyltransferases involved in the synthesis of the lipopolysaccharide (LPS) glycan (15). Counterselection on M9S-rhamnose plates yielded single colonies, all tetracycline sensitive. PCR analysis demonstrated that of 10 resolvents analyzed, 2 were deletion mutants (clones 8 and 9) (Fig. 4E). We further verified the phenotype of this deletion mutant by Western immunoblotting of whole-cell lysates using an antiserum specific to the LPS glycan of *Bv*CL10 (15). The antibody reactivity to this glycan is lost in the Δ*CK234_00400-1* mutant (Fig. 4E), providing phenotypic confirmation of the deletion.

To further increase the breadth of strains that can be mutated and the genetic pool to include allelic replacement of genes in tetracycline-inducible CTns, we created pLGB31 (Fig. 4F). This vector is similar to pLGB29 in that cointegrates are selected by the acquisition of inulin utilization but with rhamnose as the inducer of *ssbfe1* for selection of double-crossover resolvents.

In summary, we have created a versatile family of vectors and protocols to greatly facilitate genetic manipulation of diverse *Bacteroides* and *Parabacteroides* strains. These vectors allow for allelic deletions and replacements in the increasingly abundant antibiotic-resistant strains that are currently not amenable to genetic manipulation with existing genetic tools. Routine mutant construction times are reduced from several weeks to less than 2 weeks, and the steps are much less labor-intensive than protocols without counterselection. In addition, there is no need to create a mutant background strain for counterselection. Bfe1 is a broad-range and potent toxin, and we have not encountered instances of spontaneous resistance mutations in any species. This is an easily modifiable system where the ssBfe1 toxin gene could be exchanged for a different GA3 T6SS toxin gene for genetic manipulation in *B. fragilis* strains, such as 638R, that encode the cognate immunity protein Bfi1. The versatility of two different inducers of Bfe1 increases the breadth of strains and genes that can be genetically manipulated.

FIG 4 Legend (Continued)
resistance gene. (C, top) PCR verification of the cointegrates and counterselected clones for the *ubb* deletion in *Bf*9343, using primers 1 and 2, as indicated in the Fig. 2A legend. WT, wild type; CI, cointegrate; C−, no-DNA control; MW, molecular weight marker. (Bottom) Overlay assays to test BfUbb inhibitory activity by wild-type or Δ*ubb Bf*9343, using the specified strains as indicators and producers. (D) Growth curves of the specified *B. fragilis* strains containing a chromosomally integrated rhamnose-inducible *ssbfe1*. Black arrows indicate the timing of rhamnose addition to the culture. The means and SEM from 3 biological replicates per treatment are plotted. (E, left) PCR verification of the counterselected clones for the deletion of *CK234_00400-1* in *Bv*CL10, using primers 1 and 2, as indicated in the Fig. 2A legend. (Right) Western immunoblotting of whole-cell lysates probed with antiserum raised to WT *Bv*CL10 adsorbed with the Δ*CK234_00400-1* mutant. (F) Allelic replacement vector pLGB31 using inulin selection. *bla*, *oriT*, RK6, and MCS are described in the Fig. 1D legend.

MATERIALS AND METHODS

Media and growth conditions. *E. coli* strains were grown aerobically at 37°C in LB medium, with 100 μg/ml carbenicillin added when indicated. *Bacteroides* and *Parabacteroides* strains were routinely grown at 37°C under anaerobic conditions on supplemented basal medium (SBM) (liquid cultures) (61) and brain heart infusion plates supplemented with 5 mg/liter hemin and 2.5 μg/liter vitamin K_1 (BHIS). When necessary for selection, M9S plates were used, which are M9 minimal medium (62) supplemented with 50 mg/liter L-cysteine, 5 mg/liter hemin, 2.5 μg/liter vitamin K_1, 2 mg/liter $FeSO_4 \cdot 7H_2O$, 5 μg/liter vitamin B_{12}, and 0.7% agarose. The carbon source for these plates was either 0.25% (wt/vol) glucose (M9S-glucose) or 0.4% (wt/vol) inulin (M9S-inulin) (inulin from chicory; Sigma-Aldrich). Antibiotics were used at the following concentrations, where appropriate: 5 μg/ml erythromycin, 200 μg/ml gentamicin, and 6 μg/ml tetracycline. Anhydrotetracycline (aTC) was added at 40 or 100 ng/ml, while L-(+)-rhamnose was used at 10 mM. For growth curves, bacteria from a culture grown overnight in broth were diluted 1:200 in fresh medium, allowed to enter exponential growth, and diluted again to an optical density at 600 nm (OD_{600}) of 0.02. Growth curves were carried out in flat-bottom 96-well plates, with 200 μl per well, under anaerobic conditions at 37°C. OD_{600} values were measured every 30 min with an Eon high-performance microplate spectrophotometer (BioTek Instruments). A total of 10 mM rhamnose was added to the corresponding wells after 3 h 35 min of incubation. The means and standard errors of the means (SEM) from 3 biological replicates per treatment were plotted in Prism 8 for macOS (GraphPad Software).

Plasmid construction. Table S1 in the supplemental material summarizes the plasmids and construction methods used in this study. Phusion high-fidelity DNA polymerase or Q5 high-fidelity DNA polymerase was used for PCR cloning steps (New England Biolabs [NEB]), and all restriction endonucleases were high-fidelity restriction endonucleases from NEB. All plasmid assembly reactions were carried out using NEBuilder HiFi DNA assembly master mix (NEB). Oligonucleotides used for plasmid construction and PCR strain verification are listed in Table S2. Whole-plasmid sequencing was performed at the Massachusetts General Hospital CCIB DNA Core. The inulin utilization cassette causes a fitness defect in *E. coli*, leading to colonies that are smaller and more mucoid than the wild type and take 24 h to appear. These should be preferentially picked over the faster-appearing, nonmucoid colonies, which are likely to carry loss-of-function mutations. In order to avoid accumulation of mutations in the inulin plasmid, we recommend minimizing propagation steps and working on a Tn*10*-negative cloning strain.

Conjugation and selection conditions. Parental strains and strains constructed in this study are listed in Table S3. Plasmids were transformed into the donor *E. coli* strain S17-*λpir* and conjugated into *Bacteroides* or *Parabacteroides* as described previously (31, 63), with some modifications. Briefly, donor and recipient strains were grown on liquid medium, 25 ml and 2.5 ml, respectively. When the recipient strain reached an OD_{600} of between 0.1 and 0.2 (0.05 for *B. fragilis*) and the donor strain reached an OD_{600} of 0.2 to 0.6, both strains were mixed and pelleted by centrifugation at 9,000 $\times$ *g* for 10 min. The pellet was resuspended in 100 μl SBM, spotted directly in the center of a prewarmed BHIS plate, and incubated at 37°C aerobically for 15 to 18 h. The bacteria from the mating spot were streaked onto the appropriate selection plates (BHIS plus erythromycin, BHIS plus tetracycline, or M9S-inulin) containing gentamicin (one plate had half the mating spot, another plate had a quarter, and the last quarter of the mating spot was streaked for isolation in the third plate). For rhamnose counterselection using pLGB30 for rhamnose-utilizing strains, cointegrates were selected using M9S-glucose plates with gentamicin and tetracycline. Plates were incubated anaerobically. Colonies were picked after 2 to 3 days (BHIS and M9S-glucose) or 3 to 4 days (M9S-inulin) and restreaked for isolation. PCRs for strain verification were performed using Phusion DNA polymerase with the oligonucleotides listed in Table S2.

Counterselection conditions. After confirmation of cointegrates via PCR (Table S2), each strain was grown overnight in 6 ml SBM, diluted 1:100 in fresh SBM, and incubated for 6 to 8 h. Aliquots of 50, 5, 1, and 0.2 μl were plated onto BHIS plates containing 40 or 100 ng/ml aTC or 10 mM rhamnose, depending on the selection method. We have found that cointegrates can be grown from plates in nonselective medium for as little as an hour before plating for counterselection, eliminating the need for culture overnight. For rhamnose counterselection in rhamnose-utilizing strains, bacteria were grown in M9S-glucose broth and plated onto M9S-rhamnose (10 mM). After 2 to 4 days, single colonies were restreaked and analyzed by PCR to confirm the loss of the selection marker (Table S2).

Agar overlay assays. Agar spot overlay assays were carried out as previously described (30). Briefly, 5 μl of the toxin-producing strain or mutant was spotted onto plates and incubated overnight anaerobically. Cells were removed, and the plates were exposed to chloroform vapor to kill remaining bacteria. The overlay strain was grown to exponential phase, added to 4 ml warm BHIS with 0.8% agar, and poured on top of the chloroform-treated plate. Plates were incubated overnight anaerobically before imaging.

Western blot analyses. Western immunoblot analyses of exponential-phase cell lysates were performed as described previously, using antiserum prepared in rabbits to whole-cell *B. vulgatus* CL10T00C06, and subjected to antibody adsorption to *B. vulgatus* CL10T00C06 Δ*CK234_00400-1* (15).

Data availability. The vectors created in this study can be acquired from the Addgene repository (ID numbers 126617 to 126621; https://www.addgene.org/browse/article/28203359/).

SUPPLEMENTAL MATERIAL

Supplemental material for this article may be found at https://doi.org/10.1128/mBio.01762-19.

TABLE S1, PDF file, 0.04 MB.

TABLE S2, PDF file, 0.03 MB.

TABLE S3, PDF file, 0.04 MB.

ACKNOWLEDGMENTS

We thank Michael Coyne and Juan Vasquez for discussions and critical comments on the manuscript. We are grateful to members of the Comstock lab for technical assistance, in particular Hongxia Bao for identifying *P. merdae* tractable strains. We thank Andrew Goodman for providing vector pNBU2_erm-TetR-P1T_DP-GH023 and Mark Mimee for multiple vectors and helpful discussions.

This work was supported by Public Health Service grant R01AI120633 from the National Institutes of Health/National Institute of Allergy and Infectious Diseases. The funders had no role in study design, data collection and interpretation, or the decision to submit the work for publication.

We declare no conflicts of interest.

REFERENCES

1. Kundu P, Blacher E, Elinav E, Pettersson S. 2017. Our gut microbiome: the evolving inner self. Cell 171:1481–1493. https://doi.org/10.1016/j.cell.2017.11.024.
2. McKenney PT, Pamer EG. 2015. From hype to hope: the gut microbiota in enteric infectious disease. Cell 163:1326–1332. https://doi.org/10.1016/j.cell.2015.11.032.
3. Heintz-Buschart A, Wilmes P. 2018. Human gut microbiome: function matters. Trends Microbiol 26:563–574. https://doi.org/10.1016/j.tim.2017.11.002.
4. Taroncher-Oldenburg G, Jones S, Blaser M, Bonneau R, Christey P, Clemente JC, Elinav E, Ghedin E, Huttenhower C, Kelly D, Kyle D, Littman D, Maiti A, Maue A, Olle B, Segal L, van Hylckama Vlieg JET, Wang J. 2018. Translating microbiome futures. Nat Biotechnol 36:1037–1042. https://doi.org/10.1038/nbt.4287.
5. Human Microbiome Project Consortium. 2012. Structure, function and diversity of the healthy human microbiome. Nature 486:207–214. https://doi.org/10.1038/nature11234.
6. Pasolli E, Asnicar F, Manara S, Zolfo M, Karcher N, Armanini F, Beghini F, Manghi P, Tett A, Ghensi P, Collado MC, Rice BL, DuLong C, Morgan XC, Golden CD, Quince C, Huttenhower C, Segata N. 2019. Extensive unexplored human microbiome diversity revealed by over 150,000 genomes from metagenomes spanning age, geography, and lifestyle. Cell 176:649.e20–662.e20. https://doi.org/10.1016/j.cell.2019.01.001.
7. Faith JJ, Guruge JL, Charbonneau M, Subramanian S, Seedorf H, Goodman AL, Clemente JC, Knight R, Heath AC, Leibel RL, Rosenbaum M, Gordon JI. 2013. The long-term stability of the human gut microbiota. Science 341:1237439. https://doi.org/10.1126/science.1237439.
8. Mehta RS, Abu-Ali GS, Drew DA, Lloyd-Price J, Subramanian A, Lochhead P, Joshi AD, Ivey KL, Khalili H, Brown GT, DuLong C, Song M, Nguyen LH, Mallick H, Rimm EB, Izard J, Huttenhower C, Chan AT. 2018. Stability of the human faecal microbiome in a cohort of adult men. Nat Microbiol 3:347–355. https://doi.org/10.1038/s41564-017-0096-0.
9. Lloyd-Price J, Mahurkar A, Rahnavard G, Crabtree J, Orvis J, Hall AB, Brady A, Creasy HH, McCracken C, Giglio MG, McDonald D, Franzosa EA, Knight R, White O, Huttenhower C. 2017. Strains, functions and dynamics in the expanded Human Microbiome Project. Nature 550:61–66. https://doi.org/10.1038/nature24485.
10. Wexler AG, Goodman AL. 2017. An insider's perspective: *Bacteroides* as a window into the microbiome. Nat Microbiol 2:17026. https://doi.org/10.1038/nmicrobiol.2017.26.
11. Salyers AA, Bonheyo G, Shoemaker NB. 2000. Starting a new genetic system: lessons from *Bacteroides*. Methods 20:35–46. https://doi.org/10.1006/meth.1999.0903.
12. Lange A, Beier S, Steimle A, Autenrieth IB, Huson DH, Frick J-S. 2016. Extensive mobilome-driven genome diversification in mouse gut-associated *Bacteroides vulgatus* mpk. Genome Biol Evol 8:1197–1207. https://doi.org/10.1093/gbe/evw070.
13. Husain F, Tang K, Veeranagouda Y, Boente R, Patrick S, Blakely G, Wexler HM. 14 November 2017. Novel large-scale chromosomal transfer in *Bacteroides fragilis* contributes to its pan-genome and rapid environmental adaptation. Microb Genomics https://doi.org/10.1099/mgen.0.000136.
14. Coyne MJ, Comstock LE. 2019. Type VI secretion systems and the gut microbiota. Microbiol Spectr 7:PSIB-0009-2018. https://doi.org/10.1128/microbiolspec.PSIB-0009-2018.
15. McEneany VL, Coyne MJ, Chatzidaki-Livanis M, Comstock LE. 2018. Acquisition of MACPF domain-encoding genes is the main contributor to LPS glycan diversity in gut *Bacteroides* species. ISME J 12:2919–2928. https://doi.org/10.1038/s41396-018-0244-4.
16. Coyne MJ, Roelofs KG, Comstock LE. 2016. Type VI secretion systems of human gut Bacteroidales segregate into three genetic architectures, two of which are contained on mobile genetic elements. BMC Genomics 17:58. https://doi.org/10.1186/s12864-016-2377-z.
17. Coyne MJ, Zitomersky NL, McGuire AM, Earl AM, Comstock LE. 2014. Evidence of extensive DNA transfer between Bacteroidales species within the human gut. mBio 5:e01305-14. https://doi.org/10.1128/mBio.01305-14.
18. Zitomersky NL, Coyne MJ, Comstock LE. 2011. Longitudinal analysis of the prevalence, maintenance, and IgA response to species of the order Bacteroidales in the human gut. Infect Immun 79:2012–2020. https://doi.org/10.1128/IAI.01348-10.
19. Casterline BW, Hecht AL, Choi VM, Bubeck Wardenburg J. 2017. The *Bacteroides fragilis* pathogenicity island links virulence and strain competition. Gut Microbes 8:374–383. https://doi.org/10.1080/19490976.2017.1290758.
20. Joglekar P, Sonnenburg ED, Higginbottom SK, Earle KA, Morland C, Shapiro-Ward S, Bolam DN, Sonnenburg JL. 2018. Genetic variation of the SusC/SusD homologs from a polysaccharide utilization locus underlies divergent fructan specificities and functional adaptation in *Bacteroides thetaiotaomicron* strains. mSphere 3:e00185-18. https://doi.org/10.1128/mSphereDirect.00185-18.
21. Boente RF, Ferreira LQ, Falcão LS, Miranda KR, Guimarães PLS, Santos-Filho J, Vieira JMBD, Barroso DE, Emond J-P, Ferreira EO, Paula GR, Domingues RMCP. 2010. Detection of resistance genes and susceptibility patterns in *Bacteroides* and *Parabacteroides* strains. Anaerobe 16:190–194. https://doi.org/10.1016/j.anaerobe.2010.02.003.
22. Boyanova L, Kolarov R, Mitov I. 2015. Recent evolution of antibiotic resistance in the anaerobes as compared to previous decades. Anaerobe 31:4–10. https://doi.org/10.1016/j.anaerobe.2014.05.004.
23. Snydman DR, Jacobus NV, McDermott LA, Goldstein EJC, Harrell L, Jenkins SG, Newton D, Patel R, Hecht DW. 2017. Trends in antimicrobial resistance among *Bacteroides* species and *Parabacteroides* species in the United States from 2010–2012 with comparison to 2008–2009. Anaerobe 43:21–26. https://doi.org/10.1016/j.anaerobe.2016.11.003.
24. Hastey CJ, Boyd H, Schuetz AN, Anderson K, Citron DM, Dzink-Fox J, Hackel M, Hecht DW, Jacobus NV, Jenkins SG, Karlsson M, Knapp CC, Koeth LM, Wexler H, Roe-Carpenter DE. 2016. Changes in the antibiotic susceptibility of anaerobic bacteria from 2007–2009 to 2010–2012 based on the CLSI methodology. Anaerobe 42:27–30. https://doi.org/10.1016/j.anaerobe.2016.07.003.
25. Whittle G, Shoemaker NB, Salyers AA. 2002. The role of *Bacteroides* conjugative transposons in the dissemination of antibiotic resistance genes. Cell Mol Life Sci 59:2044–2054. https://doi.org/10.1007/s000180200004.
26. Nagy E, Urbán E, Nord CE. 2011. Antimicrobial susceptibility of *Bacteroides fragilis* group isolates in Europe: 20 years of experience. Clin Microbiol Infect 17:371–379. https://doi.org/10.1111/j.1469-0691.2010.03256.x.
27. Wexler HM. 2007. *Bacteroides*: the good, the bad, and the nitty-gritty. Clin Microbiol Rev 20:593–621. https://doi.org/10.1128/CMR.00008-07.

28. Hecht DW. 2006. Anaerobes: antibiotic resistance, clinical significance, and the role of susceptibility testing. Anaerobe 12:115–121. https://doi.org/10.1016/j.anaerobe.2005.10.004.
29. Bacic MK, Smith CJ. 2008. Laboratory maintenance and cultivation of *Bacteroides* species. Curr Protoc Microbiol Chapter 13:Unit 13C.1. https://doi.org/10.1002/9780471729259.mc13c01s9.
30. Roelofs KG, Coyne MJ, Gentyala RR, Chatzidaki-Livanis M, Comstock LE. 2016. Bacteroidales secreted antimicrobial proteins target surface molecules necessary for gut colonization and mediate competition in vivo. mBio 7:e01055-16. https://doi.org/10.1128/mBio.01055-16.
31. Salyers AA, Shoemaker N, Cooper A, D'Elia J, Shipman JA. 1999. 8 genetic methods for *Bacteroides* species. Methods Microbiol 29:229–249. https://doi.org/10.1016/S0580-9517(08)70119-3.
32. Smith CJ, Rogers MB, McKee ML. 1992. Heterologous gene expression in *Bacteroides fragilis*. Plasmid 27:141–154. https://doi.org/10.1016/0147-619X(92)90014-2.
33. Park J, Salyers AA. 2011. Characterization of the *Bacteroides* CTnDOT regulatory protein RteC. J Bacteriol 193:91–97. https://doi.org/10.1128/JB.01015-10.
34. Teixeira FL, Pauer H, Costa SB, Smith CJ, Domingues RMCP, Rocha ER, Lobo LA. 2018. Deletion of BmoR affects the expression of genes related to thiol/disulfide balance in *Bacteroides fragilis*. Sci Rep 8:14405. https://doi.org/10.1038/s41598-018-32880-7.
35. Betteken MI, Rocha ER, Smith CJ. 2015. Dps and DpsL mediate survival *in vitro* and *in vivo* during the prolonged oxidative stress response in *Bacteroides fragilis*. J Bacteriol 197:3329–3338. https://doi.org/10.1128/JB.00342-15.
36. Sutanto Y, DiChiara JM, Shoemaker NB, Gardner JF, Salyers AA. 2004. Factors required in vitro for excision of the *Bacteroides* conjugative transposon, CTnDOT. Plasmid 52:119–130. https://doi.org/10.1016/j.plasmid.2004.06.003.
37. Ruppé É, Woerther P-L, Barbier F. 2015. Mechanisms of antimicrobial resistance in Gram-negative bacilli. Ann Intensive Care 5:21. https://doi.org/10.1186/s13613-015-0061-0.
38. Peters JM, Silvis MR, Zhao D, Hawkins JS, Gross CA, Qi LS. 2015. Bacterial CRISPR: accomplishments and prospects. Curr Opin Microbiol 27:121–126. https://doi.org/10.1016/j.mib.2015.08.007.
39. Selle K, Barrangou R. 2015. Harnessing CRISPR-Cas systems for bacterial genome editing. Trends Microbiol 23:225–232. https://doi.org/10.1016/j.tim.2015.01.008.
40. Arazoe T, Kondo A, Nishida K. 2018. Targeted nucleotide editing technologies for microbial metabolic engineering. Biotechnol J 13:e1700596. https://doi.org/10.1002/biot.201700596.
41. Ichimura M, Nakayama-Imaohji H, Wakimoto S, Morita H, Hayashi T, Kuwahara T. 2010. Efficient electrotransformation of *Bacteroides fragilis*. Appl Environ Microbiol 76:3325–3332. https://doi.org/10.1128/AEM.02420-09.
42. Lazarus JE, Warr AR, Kuehl CJ, Giorgio RT, Davis BM, Waldor MK. 14 June 2019. A new suite of allelic exchange vectors for the scarless modification of proteobacterial genomes. Appl Environ Microbiol https://doi.org/10.1128/AEM.00990-19.
43. Kino Y, Nakayama-Imaohji H, Fujita M, Tada A, Yoneda S, Murakami K, Hashimoto M, Hayashi T, Okazaki K, Kuwahara T. 2016. Counterselection employing mutated pheS for markerless genetic deletion in *Bacteroides* species. Anaerobe 42:81–88. https://doi.org/10.1016/j.anaerobe.2016.09.004.
44. Rakoff-Nahoum S, Foster KR, Comstock LE. 2016. The evolution of cooperation within the gut microbiota. Nature 533:255–259. https://doi.org/10.1038/nature17626.
45. Martens EC, Chiang HC, Gordon JI. 2008. Mucosal glycan foraging enhances fitness and transmission of a saccharolytic human gut bacterial symbiont. Cell Host Microbe 4:447–457. https://doi.org/10.1016/j.chom.2008.09.007.
46. Martens EC, Koropatkin NM, Smith TJ, Gordon JI. 2009. Complex glycan catabolism by the human gut microbiota: the Bacteroidetes Sus-like paradigm. J Biol Chem 284:24673–24677. https://doi.org/10.1074/jbc.R109.022848.
47. Sonnenburg ED, Zheng H, Joglekar P, Higginbottom SK, Firbank SJ, Bolam DN, Sonnenburg JL. 2010. Specificity of polysaccharide use in intestinal *Bacteroides* species determines diet-induced microbiota alterations. Cell 141:1241–1252. https://doi.org/10.1016/j.cell.2010.05.005.
48. Rakoff-Nahoum S, Coyne MJ, Comstock LE. 2014. An ecological network of polysaccharide utilization among human intestinal symbionts. Curr Biol 24:40–49. https://doi.org/10.1016/j.cub.2013.10.077.
49. Vingadassalom D, Kolb A, Mayer C, Rybkine T, Collatz E, Podglajen I. 2005. An unusual primary sigma factor in the Bacteroidetes phylum: primary sigma factor of *Bacteroides fragilis*. Mol Microbiol 56:888–902. https://doi.org/10.1111/j.1365-2958.2005.04590.x.
50. Koropatkin NM, Martens EC, Gordon JI, Smith TJ. 2008. Starch catabolism by a prominent human gut symbiont is directed by the recognition of amylose helices. Structure 16:1105–1115. https://doi.org/10.1016/j.str.2008.03.017.
51. Wang J, Shoemaker NB, Wang G-R, Salyers AA. 2000. Characterization of a *Bacteroides* mobilizable transposon, NBU2, which carries a functional lincomycin resistance gene. J Bacteriol 182:3559–3571. https://doi.org/10.1128/jb.182.12.3559-3571.2000.
52. Chatzidaki-Livanis M, Geva-Zatorsky N, Comstock LE. 2016. *Bacteroides fragilis* type VI secretion systems use novel effector and immunity proteins to antagonize human gut Bacteroidales species. Proc Natl Acad Sci U S A 113:3627–3632. https://doi.org/10.1073/pnas.1522510113.
53. Lim B, Zimmermann M, Barry NA, Goodman AL. 2017. Engineered regulatory systems modulate gene expression of human commensals in the gut. Cell 169:547.e15–558.e15. https://doi.org/10.1016/j.cell.2017.03.045.
54. Ross BD, Verster AJ, Radey MC, Schmidtke DT, Pope CE, Hoffman LR, Hajjar A, Peterson SB, Borenstein E, Mougous J. 2018. Acquired interbacterial defense systems protect against interspecies antagonism in the human gut microbiome. bioRxiv https://doi.org/10.1101/471110.
55. Bacic M, Parker AC, Stagg J, Whitley HP, Wells WG, Jacob LA, Smith CJ. 2005. Genetic and structural analysis of the *Bacteroides* conjugative transposon CTn341. J Bacteriol 187:2858–2869. https://doi.org/10.1128/JB.187.8.2858-2869.2005.
56. Peed L, Parker AC, Smith CJ. 2010. Genetic and functional analyses of the mob operon on conjugative transposon CTn341 from *Bacteroides spp*. J Bacteriol 192:4643–4650. https://doi.org/10.1128/JB.00317-10.
57. Mimee M, Tucker AC, Voigt CA, Lu TK. 2015. Programming a human commensal bacterium, *Bacteroides thetaiotaomicron*, to sense and respond to stimuli in the murine gut microbiota. Cell Syst 1:62–71. https://doi.org/10.1016/j.cels.2015.06.001.
58. Patel EH, Paul LV, Patrick S, Abratt VR. 2008. Rhamnose catabolism in *Bacteroides thetaiotaomicron* is controlled by the positive transcriptional regulator RhaR. Res Microbiol 159:678–684. https://doi.org/10.1016/j.resmic.2008.09.002.
59. Chatzidaki-Livanis M, Coyne MJ, Roelofs KG, Gentyala RR, Caldwell JM, Comstock LE. 2017. Gut symbiont *Bacteroides fragilis* secretes a eukaryotic-like ubiquitin protein that mediates intraspecies antagonism. mBio 8:e01902-17. https://doi.org/10.1128/mBio.01902-17.
60. Shumaker AM, Laclare McEneany V, Coyne MJ, Silver PA, Comstock LE. 2019. Identification of a fifth antibacterial toxin produced by a single *Bacteroides fragilis* strain. J Bacteriol 201:e00577-18. https://doi.org/10.1128/JB.00577-18.
61. Pantosti A, Tzianabos AO, Onderdonk AB, Kasper DL. 1991. Immunochemical characterization of two surface polysaccharides of *Bacteroides fragilis*. Infect Immun 59:2075–2082.
62. Sambrook J, Fritsch EF, Maniatis T. 1989. Molecular cloning: a laboratory manual, 2nd ed. Cold Spring Harbor Laboratory Press, Cold Spring Harbor, NY.
63. Shoemaker NB, Getty C, Guthrie EP, Salyers AA. 1986. Regions in *Bacteroides* plasmids pBFTM10 and pB8-51 that allow Escherichia coli-Bacteroides shuttle vectors to be mobilized by IncP plasmids and by a conjugative Bacteroides tetracycline resistance element. J Bacteriol 166:959–965. https://doi.org/10.1128/jb.166.3.959-965.1986.
64. Baughn AD, Malamy MH. 2002. A mitochondrial-like aconitase in the bacterium *Bacteroides fragilis*: implications for the evolution of the mitochondrial Krebs cycle. Proc Natl Acad Sci U S A 99:4662–4667. https://doi.org/10.1073/pnas.052710199.
65. Coyne MJ, Béchon N, Matano LM, Laclare McEneany V, Chatzidaki-Livanis M, Comstock LE. 2019. A family of anti-Bacteroidales peptide toxins wide-spread in the human gut microbiota. Nat Commun 10:3460. https://doi.org/10.1038/s41467-019-11494-1.